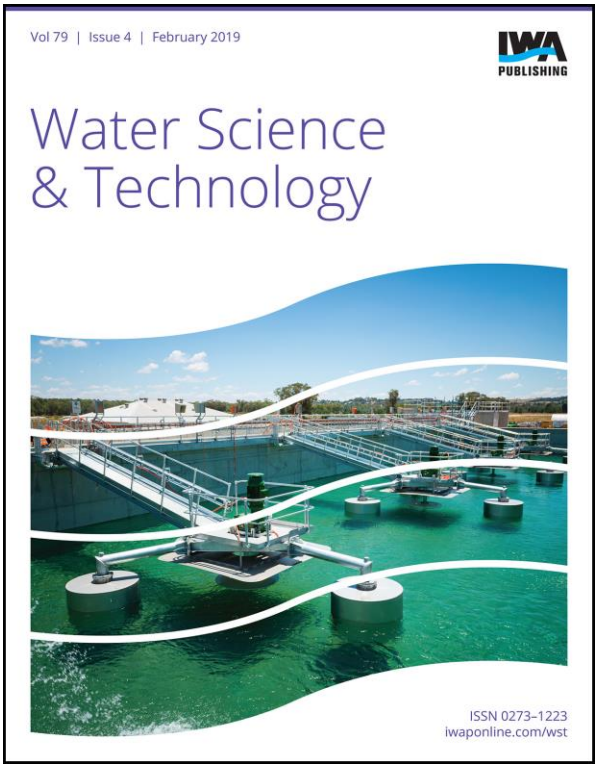

Biosorption of crystal violet dye using inactive biomass of the fungus *Diaporthe schini*

Patrícia Grassi, Caroline Reis, Fernanda C. Drumm, Jordana Georgin, Denise Tonato, Leticia B. Escudero, Raquel Kuhn, Sérgio L. Jahn and Guilherme L. Dotto

ABSTRACT

An inactive biomass of a new fungus recently discovered, *Diaporthe schini*, was evaluated for the biosorption of crystal violet (CV) in simulated textile effluents. The characterization assays were performed using X-ray diffraction (XRD), Fourier transform infrared spectroscopy (FTIR), scanning electron microscopy (SEM) and N_2 adsorption/desorption isotherms. The influences of pH and biosorbent dosage on the biosorption capacity were evaluated. Kinetics, equilibrium and thermodynamic studies were also carried out. Characterization techniques showed an amorphous biosorbent, with a rough surface containing irregular particles and surface area of 6.5 $m^2 g^{-1}$. The most adequate values of pH and biosorbent dosage were 7.5 and 0.4 g L^{-1}, respectively. The Elovich kinetic model and the Sips equilibrium model were suitable to fit the experimental data. The biosorption capacity increased with temperature, reaching a maximum biosorption capacity of 642.3 mg g^{-1} at 328 K. The biosorption was a spontaneous and endothermic process. *Diaporthe schini* inactive biomass was an interesting biosorbent to treat colored effluents, presenting efficiency of 87% in the decolorization of a simulated dye house effluent.

Key words | biosorption, *Diaporthe schini*, fungal biomass, simulated effluent

Patrícia Grassi
Caroline Reis
Fernanda C. Drumm
Denise Tonato
Raquel Kuhn
Sérgio L. Jahn
Guilherme L. Dotto (corresponding author)
Department of Chemical Engineering,
Federal University of Santa Maria-UFSM,
1000 Roraima Avenue, Santa Maria, RS,
Brazil
E-mail: *guilherme_dotto@yahoo.com.br*

Jordana Georgin
Department of Civil Engineering,
Federal University of Santa Maria-UFSM,
1000 Roraima Avenue, Santa Maria, RS,
Brazil

Leticia B. Escudero
Faculty of Natural and Exact Sciences,
National University of Cuyo,
Padre J. Contreras 1300, 5500 Mendoza,
Argentina

INTRODUCTION

The discharge of synthetic dyes in industrial effluents is a topic of growing concern due to their high polluting potential. It is estimated that approximately 280,000 tons of these compounds are annually disposed of in an environmentally inadequate manner (Sen *et al.* 2016). The presence of dyes in the environment causes serious risks, since they hinder the incidence of solar radiation, damaging the development of the existing biota. Moreover, the presence of dyes in wastewater is a problem due to their toxic, carcinogenic and teratogenic character (Naskar & Majumder 2017). Therefore, efficient treatments are necessary to allow the removal of these contaminants from wastewater before release into the environment (Fabryanty *et al.* 2017).

Several processes are used on an industrial scale to remove contaminants from aqueous effluents. Adsorption/biosorption, advanced oxidative processes, coagulation, ion exchange, and membrane filtration are some examples of operations usually used. Adsorption is considered one of the most promising alternatives for the removal of organic molecules due to its simplicity, low cost and high removal efficiency (Gopi *et al.* 2016). Activated carbon is the most commonly used adsorbent for dye removal. However, its use is limited because of the high cost. In this way, the scientific community has sought the use of alternative adsorbents that, besides allowing the efficient removal of contaminants, have a low cost of acquisition (Naskar & Majumder 2017). Thus, residues or byproducts from industrial processes are excellent materials. Among these alternatives, the use of biomass generated in fermentative processes using bacteria (Luo *et al.* 2014) and fungi cells (Puchana-Rosero *et al.* 2017; Li *et al.* 2018) can be highlighted.

In fermentative processes, large amounts of biomass are generated for the production of different products. After extraction of the desired compounds, the wastes must be discarded, offering great potential to be exploited as low cost biosorbents (Svecova *et al.* 2006). Fungi used in

doi: 10.2166/wst.2019.091

fermentative processes present in their cell walls compounds including polysaccharides (mainly chitin), lipids, proteins, and pigments in minor proportion (Escudero *et al.* 2018), which provide a variety of functional groups that can favor the biosorption process. Fermentative processes using fungi of the *Diaporthe* genus have been used in the production of secondary metabolites, which have been applied in different fields according to their antibacterial, anticancer, antifungal, antimalarial, antiviral, cytotoxic and herbicidal activity (Guarnaccia *et al.* 2018). To date, no studies have been reported in the scientific literature related to physicochemical characterization and application of the inactive biomass of *Diaporthe schini* fungus as a biosorbent for removal of contaminants. The use of this byproduct (inactive biomass), generated in biotechnological processes of production of secondary metabolites, would be an alternative to valorize the byproduct and reduce costs for obtaining the biomass. Therefore, this work aims to characterize the inactive biomass generated in the fermentation process of the *Diaporthe schini* fungus and to evaluate its biosorption potential for the removal of crystal violet (CV) dye.

MATERIALS AND METHODS

Preparation of the fungal biosorbent

The biomass of the fungus *Diaporthe schini* was obtained by submerged fermentation, where the main objective was the production of secondary metabolites for *in vitro* evaluation of the antimicrobial and antifungal activity. The fermentation conditions and composition of the medium followed the parameters optimized in a previous work (Souza *et al.* 2015). After fermentation, the biomass was separated from the fermentation broth by centrifugation (Eppendorf, 5804R, Brazil) for 10 min at 4,000 rpm. The broth followed for later extraction processes of the compounds for further evaluation of the antimicrobial and antifungal activity, while the residual biomass was used for biosorption studies. The resulting solid was oven dried at 100 °C for a period of 24 h to inactivate the microorganism. Finally, the biomass was macerated, sifted in a 0.25 mm (60 mesh) sieve and packed into a container.

Characterization of *Diaporthe schini* inactive biomass

The point of zero charge (pH_{pzc}) of the fungal biomass was determined by a method previously described (Postai *et al.* 2016): 0.05 g of fungal biomass was conditioned in 11 Erlenmeyer flasks, to which were added 20 mL of NaCl solution (0.1 mol L^{-1}). The pH of the solutions was adjusted to 2, 3, 4, 5, 6, 7, 8, 9, 10, 11 and 12 using HCl (0.1 mol L^{-1}) or NaOH (0.1 mol L^{-1}) solutions and kept under stirring for 24 hours at 150 rpm and 25 °C. Then, the samples were filtered and the final pH of the solution was determined using pre-calibrated digital ion mark pH. For each pH value assayed, the value of ΔpH was determined as the difference between the initial and final pH values ($\Delta pH = pH_i - pH_f$). The pH_{pzc} was defined as the point where the value of $\Delta pH = 0$ (zero), on the graph ΔpH *vs* pH*i*. The biosorbent was characterized by X-ray diffraction (XRD) using a Rigaku Mini flex model 300 diffractometer, operated with Cu-Kα radiation ($\lambda = 1.5418$ Å), 30 kV, 10 mA, step size of 0.03 and a count time of 0.5 s per step. The functional groups present in the sample were identified by Fourier transform infrared spectroscopy (FTIR) (Prestige, 21210045, Japan) in the range of 400–4,000 cm^{-1}. The specific surface area, pore volume and pore size distribution were determined by adsorption/desorption of N_2 (ASAP 2020, Micromeritics). The specific surface area was determined based on the Brunauer-Emmett-Teller (BET) method and the pore volume and pore size distribution by the Barrett-Joyner-Halenda (BJH) method. The biosorbent morphology was verified using scanning electron microscopy (SEM) (Tescan, Vega, Czech Republic).

Biosorption assays

CV dye was used as the contaminant for the biosorption studies. The dye characteristics are: color index 42555, molar weight = 407.98 g mol^{-1}, $\lambda_{max} = 590$ nm, purity = 99.0%. CV was purchased from INLAB Ltda (Brazil).

Different concentrations of CV were obtained from dilution of the stock solution (1.0 g L^{-1}) with distilled water. A calibration curve was generated in order to determine the concentration of the dye present in the solution as a function of the absorbance. The absorbance of the solutions was determined using an UV/Vis spectrophotometer (Biospectro SP-22, Brazil), at the maximum dye wavelength ($\lambda = 590$ nm). The volume of solution used in the biosorption experiments was 50 mL, kept in Erlenmeyer flasks, with stirring at 150 rpm (Marconi, MA 093, Brazil). Removal of the biosorbent from the medium was performed by centrifugation (Centribio, 80-2B, Brazil) at 4,000 rpm for 10 min. The effect of pH (2-10) was initially evaluated by keeping the mass biosorbent, CV dye concentration, biosorption temperature and time at 1.5 g L^{-1}, 100 mg L^{-1}, 298 K

and 120 min, respectively. The biosorbent dosage effect was then evaluated in the range of 0.4 to 2.0 g L^{-1}.

Under adequate pH and biosorbent dosage conditions, kinetic curves were constructed using dye concentrations of 50, 100 and 200 mg L^{-1}. Samples were collected at different time intervals up to 210 min. In each case, an initial volume of 50 mL was used and a temperature of 298 K was selected. Isotherms were constructed using the suitable conditions and equilibrium time. Four temperatures were evaluated: 298, 308, 318 and 328 K, using initial dye concentrations from 0 to 300 mg L^{-1}. The operation was evaluated according to the biosorption capacity at any time (q_t, mg g^{-1}), equilibrium biosorption capacity (q_e, mg g^{-1}) and percentage of dye removal (R, %), which were determined by simple global mass balance.

Kinetic equilibrium and thermodynamic calculations

The biosorption kinetic profile was elucidated using pseudo-first order (PFO) (Lagergren 1898), pseudo second-order (PSO) (Ho & McKay 1998) and Elovich (Wu *et al.* 2009) models. The isotherm curves were fitted by Freundlich (Freundlich 1906), Langmuir (Langmuir 1918) and Sips (Sips 1948) models. The values of standard Gibbs energy variation (ΔG°, kJ mol^{-1}), standard enthalpy change (ΔH°, kJ mol^{-1}) and standard entropy variation (ΔS°, kJ mol^{-1} K^{-1}) were also estimated (Tran *et al.* 2017). Details of kinetic, equilibrium and thermodynamic calculations are presented in the supplementary material (available with the online version of this paper).

Biosorption applied to treat a simulated textile effluent

In order to analyze the biosorption efficiency in the simulated effluent, a solution containing dyes and salts present in industrial textile effluents was prepared. The textile effluent was composed of: CV (20 mg L^{-1}), malachite green (10 mg L^{-1}), Procion red (10 mg L^{-1}), methylene blue (10 mg L^{-1}), NaCl (10 mg L^{-1}), and K_2CO_3 (10 mg L^{-1}). The biosorption assay was performed at the adequate pH and biomass dosage determined in the previous experiments, using 50 mL of simulated effluent solution under the conditions of agitation, reaction time and temperature of 150 rpm, 120 min and 298 K, respectively. Visible spectra of the effluent before and after the treatment were obtained from 300 to 800 nm using a UV–Vis spectrophotometer (Shimadzu, UV-2600, Japan). The color removal was estimated by the ratio between the areas under the spectral curves (Lima *et al.* 2017).

RESULTS AND DISCUSSION

Characteristics of *Diaporthe schini* inactive biomass

The pH_{pzc} value determined for the fungal biomass assayed was 5.4. This means that at pH above this value, the biosorbent surface will be negatively charged and could biosorb cationic molecules preferentially. In contrast, for pH values lower than pH_{pzc} the surface will be positively charged and will prefer to biosorb molecules with anionic character (Lim *et al.* 2015). So, it can be stated that *Diaporthe schini* is more suitable to uptake cationic dyes, since it is negatively charged at a wide range of pH.

Through the X-ray diffraction analysis of the fungal biomass of *Diaporthe schini* (supplementary material, Figure S1, available with the online version of this paper), it was possible to identify the appearance of a pronounced band in the range of 2θ from 20° to 35°, characteristic of an amorphous material (Naskar & Majumder 2017). This shows that the polymers present in the material have low organization, causing the appearance of the diffraction peaks characteristic of chitin or chitosan not to occur.

The infrared spectrum of the *Diaporthe schini* fungal biomass is shown in Figure 1(a). The main bands were at 3,424 cm^{-1}, which can be attributed to the stretching of O-H; 2,925 cm^{-1} attributed to the stretching of C-H bonds; 1,633 cm^{-1} and 1,550 cm^{-1} which may be attributed to the amide groups; 1,405 cm^{-1} and 1,320 cm^{-1} assigned to C-H bonds; 1,114 cm^{-1} that can be attributed to elongation of C = C and S = O; 1,088 cm^{-1} attributed to ether groups; 615 cm^{-1} attributed to the vibration elongation of C-H bonds in aromatics. The fungus showed some functional groups of natural chitin, including hydroxyl groups (OH) at 3,450 cm^{-1}, C-H at 2,960 cm^{-1}; amide groups I (carbonyl vibration C = amide stretching) and amide II (N-H deformation of amide II) at 1,650 and 1,560 cm^{-1}; CH_X deformation at 1,380 cm^{-1} and asymmetric C-O elongation at 1,020 cm^{-1}. These groups on the biosorbent surface can facilitate the dye biosorption.

The N_2 adsorption-desorption isotherm of the fungal mass of *Diaporthe schini* is shown in Figure 1(b). According to IUPAC standards, the isotherm found is classified as type II, characteristic of materials with low porosity. The surface area, volume and mean pore size determined by the BET and BJH methods were 6.5 m^2 g^{-1}, 0.02 cm^3 g^{-1} and 15.6 nm, respectively. The mean pore diameter of this type of material can be attributed to the inserts left by the cell mass formed when the fungus grows.

From the SEM analysis, it was possible to verify that the fungal biomass presented as irregular particles, of

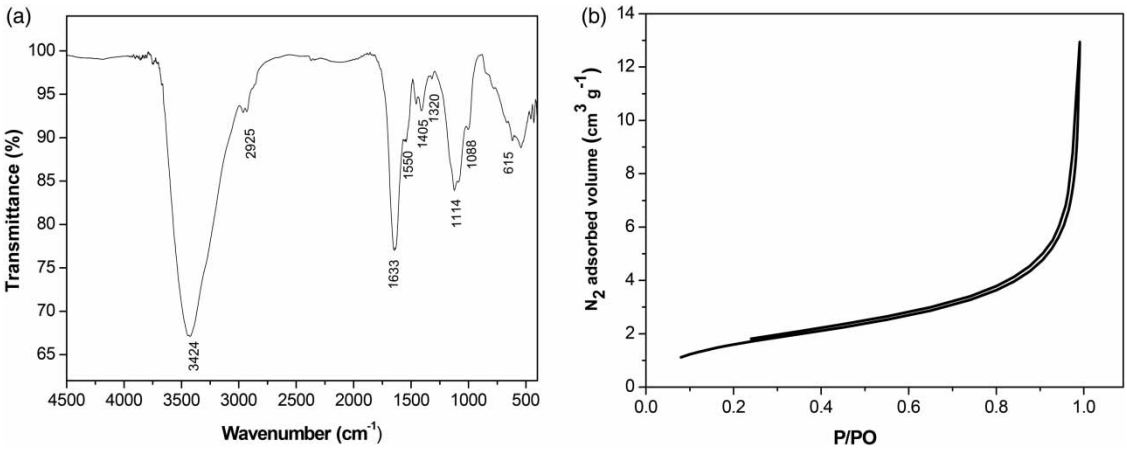

Figure 1 | (a) FT-IR vibrational spectrum of *Diaporthe schini* fungal biomass and (b) N_2 adsorption-desorption isotherm of the fungal mass.

different sizes in the range of 5 to 50 μm (Figure 2(a)). Figure 2(b) shows that the surface of these particles is quite irregular and is formed by an agglomerate of hyphae. This type of surface containing roughness and cavities is favorable to the biosorption process because it allows an interaction of the dyes in the structure of the biosorbent (Soltani *et al.* 2015).

Evaluation of pH and biosorbent dosage on the biosorption of CV

Figure 3(a) shows the effect of pH on the biosorption capacity and removal of CV dye. It can be seen that the percentage of removal increased with pH, reaching approximately 87% of dye removal at pH 6. From pH 6 to pH 10, the removal percentage was maintained at 87%. At $pH < pH_{pzc}$, the surface of the biosorbent is positively charged and CV dye is neutral or cationic (Brião *et al.* 2018). As consequence, CV and H^+ ions in the solution competes for the sites, disfavoring the cationic dye biosorption. At pH values higher than the pH_{pzc}, the biosorbent tends to be with excess of electrons in the surface, propitiating favorable conditions for cationic CV biosorption, since this dye is in its cationic form (Brião *et al.* 2018). Regarding to the biosorption capacity, higher values were found at pH higher than 6.0. Based on this information, a pH of 7.5 was selected for further experiments, since is the normal pH of the CV solution.

Figure 3(b) shows the influence of the adsorbent dosage ($g\,L^{-1}$) on the percentage of removal and biosorption capacity of the CV dye. It was found that an increase of the biosorbent dosage resulted in an increase on the

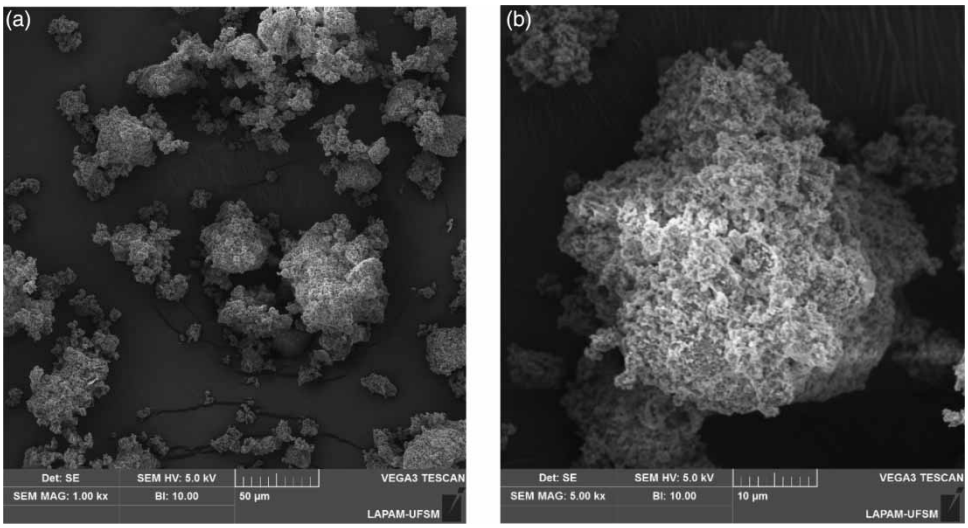

Figure 2 | Scanning electron microscopy (SEM) image of the biosorbent at magnifications of 1,000× (a) and 5,000× (b).

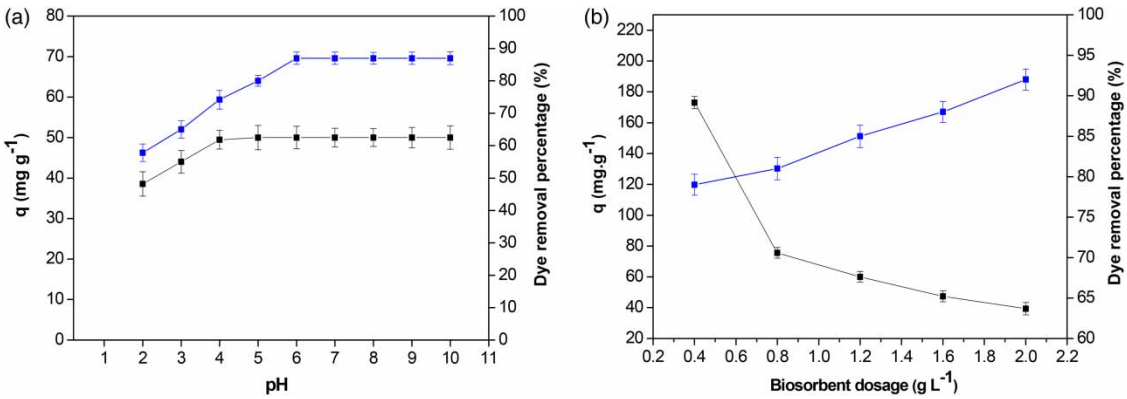

Figure 3 | (a) pH effect on the CV dye removal percentage (■) and biosorption capacity (■) by fungal biomass. (b) Biosorbent dosage effect on the dye removal percentage (■) and biosorption capacity (■) of CV dye ($V = 50$ mL, $C_0 = 100$ mg L^{-1}, $T = 298$ K).

amount of the biosorbed dye (percentage of removal) but led to a reduction in the amount of dye biosorbed per mass unit (biosorption capacity). This occurs because the number of active sites in the solid increases with increasing biosorbent dosage and therefore results in an increase in the amount of biosorbed dye. However, aggregation of these sites can occur, causing a decrease in the biosorption capacity. The highest biosorption capacity was verified when 0.4 g L^{-1} of dosage was used, corresponding to a biosorption capacity of 173.7 mg g^{-1}.

Biosorption kinetic profiles

Biosorption kinetic curves were obtained at initial dye concentrations of 50, 100 and 200 mg L^{-1}, biosorbent dosage of 0.4 g L^{-1}, temperature of 298 K and pH of 7.5. The curves are depicted in Figure 4.

An increase of the biosorption capacity can be observed until 150 minutes, maintaining constant values for longer times. This shows that the equilibrium was reached within 210 min, independent of the initial dye concentration. Moreover, when the initial dye concentration is increased, the biosorption capacity also increases, reaching a maximum value of 290 mg g^{-1}. According to other reports, this behavior is common in biosorption processes and can be attributed to two factors: (1) at higher values of initial adsorbate concentration, the concentration gradient between the solution and the outer surface of the biosorbent is higher, which facilitates the external mass transfer; (2) at higher values of initial adsorbate concentration, the diffusion surface mass flow increases (Dotto *et al.* 2014).

The pseudo-first order (PFO), pseudo-second order (PSO) and Elovich models were used to elucidate the biosorption kinetics and to obtain information about the

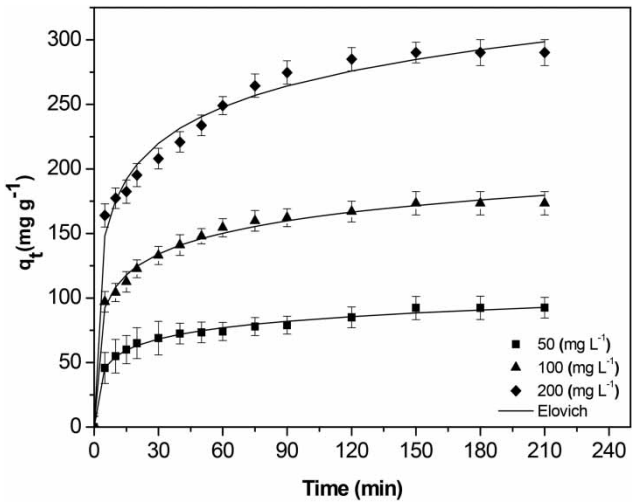

Figure 4 | Kinetic curves for CV biosorption on *Diaporthe schini* fungal biomass ($V = 500$ mL, $C_0 = 50$, 100 and 200 mg L^{-1}, biosorbent dosage = 0.4 g L^{-1}, $pH = 7.5$ and $T = 298$ K).

biosorption mechanism of the CV dye on *Diaporthe schini* fungus. The biosorption kinetic parameters are shown in Table 1.

The higher R^2 (coefficient of determination) values ($R^2 > 0.987$) and the lower ARE (average relative error) values ($ARE < 4.75\%$) presented in Table 1 show that the Elovich model was the most suitable to represent the experimental data of biosorption kinetics. In the literature, the biosorption based on the Elovich equation increases rapidly in a shorter time and, over a longer time, increases slightly (Wu *et al.* 2009). The initial velocity parameter of the Elovich model (a) increased with the initial dye concentration. This indicated that at earlier stages, the biosorption rapidly increased, mainly at higher initial CV concentrations. The b parameter decreased with the initial

Table 1 | Kinetic parameters for the CV biosorption on *Diaporthe schini* biomass

C_o (mg L^{-1})	50	100	200
PFO			
q_1 (mg g^{-1})	81.3	159.6	263.1
k_1 (min^{-1})	0.10	0.984	0.094
R^2	0.889	0.898	0.849
ARE (%)	9.22	8.45	11.01
PSO			
q_2 (mg g^{-1})	89.00	173.14	286.8
k_2 (g mg^{-1} min^{-1})	0.0016	0.0008	0.0005
R^2	0.952	0.968	0.938
ARE (%)	5.37	4.43	6.97
Elovich			
a (mg g^{-1} min^{-1})	95.0	238.5	306.9
b (g mg^{-1})	0.079	0.043	0.025
ab (min^{-1})	7.56	10.18	7.58
R^2	0.994	0.994	0.987
ARE (%)	5.14	4.73	5.52

CV concentration increase. Since the b units are g mg^{-1}, it can be concluded that adsorption capacity was higher at initial CV of 200 mg L^{-1}.

Equilibrium isotherms

Figure 5 shows the biosorption isotherms of CV dye, which were obtained at four different temperatures. The equilibrium curves were of type I (Zazycki *et al.* 2018). At low CV concentrations, an inclination was observed for all studied temperatures. This inclination shows that the fungal biomass contains available biosorption sites to uptake the CV dye. At CV concentrations higher than 200 mg L^{-1}, the isotherms tend to a plateau, indicating that all the biosorption sites were practically occupied. The results indicated that the temperature increase was favorable for the biosorption capacity of CV dye. This may occur because the increase of temperature causes a swelling effect of the fungal mass, leading to the exposure of more biosorption sites (Barbosa *et al.* 2018).

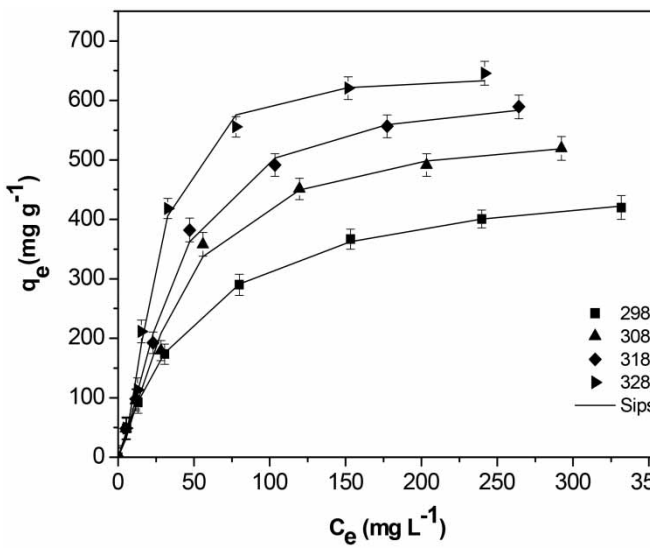

Figure 5 | Isotherm curves for CV biosorption on *Diaporthe schini* fungal biomass ($V = 50$ mL, adsorbent dosage = 0.4 g L^{-1}, pH = 7.5).

Freundlich, Langmuir and Sips models were fitted with the experimental data in order to obtain detailed information about the equilibrium. The equilibrium parameters for the biosorption of CV on the fungal biomass are presented in Table 2. From the statistical indicators (R^2, R^2_{adj} (adjusted determination coefficient) and *ARE*), it was verified that the Sips model was adequate to represent the isotherms for all temperatures. Therefore, the Sips model was selected to represent the CV dye biosorption on the fungal biomass.

Table 2 | Isotherm parameters for the biosorption of CV on *Diaporthe schini* fungal biomass

	T (K)			
Models	**298**	**308**	**318**	**328**
Freundlich				
K_F (mg g^{-1}) (mg L^{-1})$^{-1/n_F}$	41.67	49.72	53.38	72.6
$1/n_F$	0.41	0.42	0.44	0.41
R^2	0.984	0.942	0.942	0.901
R^2_{adj}	0.982	0.932	0.932	0.884
ARE (%)	17.40	27.42	31.73	44.62
Langmuir				
q_m (mg g^{-1})	494.0	633.7	728.2	787.8
K_L (L mg^{-1})	0.0178	0.0180	0.0185	0.0248
R^2	0.999	0.989	0.989	0.9705
R^2_{adj}	0.999	0.987	0.988	0.965
ARE (%)	1.30	8.04	11.60	23.75
Sips				
q_{ms} (mg g^{-1})	490.2	555.5	618.2	642.3
K_s (L mg^{-1})	0.018	0.024	0.027	0.041
m	1.040	1.353	1.434	1.865
R^2	0.999	0.994	0.997	0.994
R^2_{adj}	0.999	0.992	0.996	0.992
ARE (%)	1.40	8.90	5.95	9.25

The K_s parameter of the Sips model, which represents the equilibrium constant, increased with temperature, reaching maximum values at 328 K. This indicates that when the temperature increases, the dye affinity of the biosorbent is favored, hence increasing the biosorption capacity. The q_{mS} parameter also increased with the temperature, attaining a maximum biosorption capacity of 642.3 mg g^{-1} at 328 K. The maximum biosorption capacity is normally used to compare the potential of biosorbent/adsorbent materials to uptake dyes. Several data from the literature regarding many types of preponderantly organic materials used to remove CV dye were used for comparison with this work. This comparison is presented as supplementary material (Table S1, available online). The maximum biosorption capacity of all compared biosorbents (Table S1) ranged from 9.58 to 352.79 mg g^{-1} (Senthilkumaar *et al.* 2006; Ahmad 2009; Chakraborty *et al.* 2011; Lin *et al.* 2011; Pavan *et al.* 2014; Gopi *et al.* 2016; Muthukumaran *et al.* 2016; Sabna *et al.* 2016; Abdel-Salam *et al.* 2017; Kulkarni *et al.* 2017; Kumari *et al.* 2017; Miyah *et al.* 2017; Shoukat *et al.* 2017; Tahir *et al.* 2017; Georgin *et al.* 2018; Liu *et al.* 2018). Comparing these values with the value obtained in this work, it can be verified that the biosorption capacity of the fungal biosorbent was much higher than that verified by other authors. Coupled with the high biosorption capacity, *Diaporthe schini* fungal biomass has other advantages such as low cost, availability as fermentation waste, and biodegradability. These results show that this type of biomass has potential to be used as a biosorbent for the removal of contaminants present in liquid effluents.

Thermodynamic parameters

The biosorption thermodynamics were evaluated by the standard values of Gibbs free energy (ΔG°, kJ mol^{-1}), enthalpy (ΔH°, kJ mol^{-1}) and entropy (ΔS°, kJ mol^{-1} K^{-1}) changes. The results are shown in the supplementary material (Table S2, available online). The negative ΔG° values depicted in Table S2 indicate that the CV dye biosorption on the fungal biomass occurs spontaneously and favorably. The increase in temperature led to more negative ΔG° values, confirming that the biosorption was more favorable at 328 K. The positive value of ΔS° demonstrates that there were some rearrangements at the solid-liquid interface during the biosorption process. The positive value of ΔH° indicates that the dye biosorption is of an endothermic nature and the magnitude of ΔH° values indicates biosorption by physisorption (Barbosa *et al.* 2018).

Simulation in the treatment of a textile effluent

The *Diaporthe schini* fungal biomass was tested to treat a simulated textile effluent containing several dyes and inorganic compounds. In the test, 0.4 g L^{-1} of the biosorbent at pH 7.5 was used. Figure 6 shows the UV-visible spectra, in the range from 300 to 800 nm, before and after the biosorption process. It can be verified that there was a considerable reduction in the area under the curve, indicating that the fungal biomass was efficient in removing the color present in the simulated effluent. The percentage of removal provided in these test conditions was of the order of 86%, determined by the ratio of the area before and after biosorption. Even using low adsorbent dosage, it can be stated that the biomass of the fungus *Diaporthe schini* was very effective in the removal of a mixture of dyes and salts usually present in industrial effluents, indicating that this material presents potential to be employed as a low-cost biosorbent.

CONCLUSIONS

In this work, the potential of the inactive biomass of the fungus *Diaporthe schini* to treat colored effluents containing CV dye was demonstrated. The fungal biomass presented an amorphous character and FTIR bands similar to those observed for chitin, indicating that this polymer is part of the structure. In the SEM analysis, it was observed that the particles have varied size and irregular surface. The biosorbent material showed a BET specific area of 6.5 m^2 g^{-1}

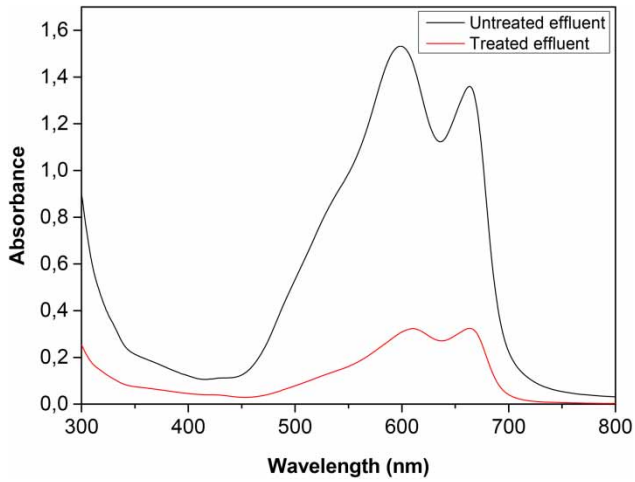

Figure 6 | Visible spectra of simulated effluent before and after treatment with fungal biomass (conditions: $V = 50$ mL, biosorbent dosage = 0.4 g L^{-1}, pH = 7.5).

and point of zero charge of 5.4. The biosorption tests showed that the maximum biosorption capacity and percentage of removal were achieved at pH of 7.5 and a biomass dosage of 0.4 g L^{-1}. The experimental data on the variation of the concentration as a function of time can be well described by the Elovich model and the equilibrium data were better represented by the Sips model. The maximum biosorption capacity was 642.3 mg g^{-1}. The thermodynamic study showed that the biosorption process of the dye on the biomass surface occurs spontaneously and is endothermic. In the experiments with simulated effluent, a color removal percentage of 87% was reached. The results showed that the biosorption process was successfully applied to a simulated effluent, predicting the great potential of this biosorbent for the removal of dyes from real industrial effluents.

REFERENCES

Abdel-Salam, A. H., Ewais, H. A. & Basaleh, A. S. 2017 Silver nanoparticles immobilised on the activated carbon as efficient adsorbent for removal of crystal violet dye from aqueous solutions. A kinetic study. *Journal of Molecular Liquids* **248** (1), 833–841.

Ahmad, R. 2009 Studies on adsorption of crystal violet dye from aqueous solution onto coniferous pinus bark powder (CPBP). *Journal of Hazardous Materials* **171** (1–3), 767–773.

Barbosa, T. R., Foletto, E. L., Dotto, G. L. & Jahn, S. L. 2018 Preparation of mesoporous geopolymer using metakaolin and rice husk ash as synthesis precursors and its use as potential adsorbent to remove organic dye from aqueous solutions. *Ceramics International* **44** (1), 416–423.

Brião, G. V., Jahn, S. L., Foletto, E. L. & Dotto, G. L. 2018 Highly efficient and reusable mesoporous zeolite synthetized from a biopolymer for cationic dyes adsorption. *Colloids and Surfaces A* **556** (1), 43–50.

Chakraborty, S., Chowdhury, S. & Das Saha, P. 2011 Adsorption of Crystal Violet from aqueous solution onto NaOH-modified rice husk. *Carbohydrate Polymers* **86** (4), 1533–1541.

Dotto, G. L., Buriol, C. & Pinto, L. A. A. 2014 Diffusional mass transfer model for the adsorption of food dyes on chitosan films. *Chemical Engineering Research and Design* **92** (1), 2324–2332.

Escudero, L. B., Quintas, P. Y., Wuilloud, R. G. & Dotto, G. L. 2018 Biosorption of metals and metalloids. In: *Green Adsorbents for Pollutant Removal 2018* (G. Crini & E. Lichtfouse, eds). Springer Nature, Basel, Switzerland, pp. 35–86.

Fabryanty, R., Valencia, C., Soetaredjo, F. E., Putro, J. N., Santoso, S. P., Kurniawan, A. & Ismadji, S. 2017 Removal of crystal violet dye by adsorption using bentonite–alginate composite. *Journal of Environmental Chemical Engineering* **5** (6), 5677–5687.

Freundlich, H. 1906 Uber die adsorption in losungen. *Zeitschrift fur Physikalische Chemie* **57** (A), 358–471.

Georgin, J., Marques, B. S., Peres, E. C., Allasia, D. & Dotto, G. L. 2018 Biosorption of cationic dyes by Pará chestnut husk (*Bertholletia excelsa*). *Water Science and Technology* **77** (6), 1612–1621.

Gopi, S., Pius, A. & Thomas, S. 2016 Enhanced adsorption of crystal violet by synthesized and characterized chitin nano whiskers from shrimp shell. *Journal of Water Process Engineering* **14** (1), 1–8.

Guarnaccia, V., Groenewald, J. Z., Woodhall, J., Armengol, J., Cinelli, T., Eichmeier, A., Ezra, D., Fontaine, F., Gramaje, D., Gutierrez-aguirregabiria, A., Kaliterna, J., Kiss, L., Larignon, P., Luque, J., Mugnai, L., Naor, V., Raposo, R., Sándor, E., Váczy, K. & Crous, P. W. 2018 Diaporthe diversity and pathogenicity revealed from a broad survey of grapevine diseases in Europe. *Persoonia* **40** (1), 135–153.

Ho, Y. S. & McKay, G. 1998 Kinetic models for the sorption of dye from aqueous solution by wood. *Process Safety and Environmental Protection* **76** (B2), 183–191.

Kulkarni, M. R., Revanth, T., Anirudh, A. & Bhat, P. 2017 Removal of Crystal Violet dye from aqueous solution using water hyacinth: equilibrium, kinetics and thermodynamics study. *Resource-Efficient Technologies* **3** (1), 71–77.

Kumari, J., Krishnamoorthy, P., Arumugam, T. K., Radhakrishnan, S. & Vasudevan, D. 2017 An efficient removal of crystal violet dye from waste water by adsorption onto TLAC/Chitosan composite: a novel low cost adsorbent. *International Journal of Biological Macromolecules* **96** (1), 324–333.

Lagergren, S. 1898 About the theory of so-called adsorption of soluble substances. *Kungliga Svenska Vetenskapsakademiens* **24** (4), 1–39.

Langmuir, I. 1918 The adsorption of gases on plane surfaces of glass, mica and platinum. *Journal of the American Chemical Society* **40** (9), 1361–1403.

Li, X., Zhang, D., Sheng, F. & Qing, H. 2018 Adsorption characteristics of Copper (II), Zinc (II) and Mercury (II) by four kinds of immobilized fungi residues. *Ecotoxicology and Environmental Safety* **147** (1), 357–366.

Lim, L. B., Priyantha, N. & Mansor, N. H. M. 2015 *Artocarpus altilis* (breadfruit) skin as a potential low-cost biosorbent for the removal of crystal violet dye: equilibrium, thermodynamics and kinetics studies. *Environmental Earth Sciences* **73** (7), 3239–3247.

Lima, D. R., Klein, L. & Dotto, G. L. 2017 Application of ultrasound modified corn straw as adsorbent for malachite green removal from synthetic and real effluents. *Environmental Science and Pollution Research* **24** (1), 21484–21495.

Lin, Y., He, X., Han, G., Tian, Q. & Hu, W. 2011 Removal of Crystal Violet from aqueous solution using powdered mycelial biomass of *Ceriporia lacerata* P2. *Journal of Environmental Sciences* **23** (12), 2055–2062.

Liu, J., Wang, Y., Fang, Y., Mwamulima, T., Song, S. & Peng, C. 2018 Removal of crystal violet and methylene blue from aqueous solutions using the fly ash-based adsorbent material-supported zero-valent iron. *Journal of Molecular Liquids* **250** (1), 468–476.

Luo, S., Li, X., Chen, L., Chen, J., Wan, Y. & Liu, C. 2014 Layer-by-layer strategy for adsorption capacity fattening of endophytic

bacterial biomass for highly effective removal of heavy metals. *Chemical Engineering Journal* **239** (1), 312–321.

Miyah, Y., Lahrichi, A., Idrissi, M., Boujraf, S., Taouda, H. & Zerrouq, F. 2017 Assessment of adsorption kinetics for removal potential of Crystal Violet dye from aqueous solutions using Moroccan pyrophyllite. *Journal of the Association of Arab Universities for Basic and Applied Sciences* **23** (1), 20–28.

Muthukumaran, C., Sivakumar, V. M. & Thirumarimurugan, M. 2016 Adsorption isotherms and kinetic studies of crystal violet dye removal from aqueous solution using surfactant modified magnetic nanoadsorbent. *Journal of the Taiwan Institute of Chemical Engineers* **63** (1), 354–362.

Naskar, A. & Majumder, R. 2017 Understanding the adsorption behaviour of acid yellow 99 on *Aspergillus niger* biomass. *Journal of Molecular Liquids* **242** (1), 892–899.

Pavan, F. A., Camacho, E. S., Lima, E. C., Dotto, G. L., Branco, V. T. A. & Dias, S. L. P. 2014 Formosa papaya seed powder (FPSP): preparation, characterization and application as an alternative adsorbent for the removal of crystal violet from aqueous phase. *Journal of Environmental Chemical Engineering* **2** (1), 230–238.

Postai, D. L., Demarchi, C. A., Zanatta, F., Melo, D. C. C. & Rodrigues, C. 2016 Adsorption of rhodamine B and methylene blue dyes using waste of seeds of *Aleurites moluccana*, a low cost adsorbent. *Alexandria Engineering Journal* **55** (2), 1713–1723.

Puchana-rosero, M. J., Lima, E. C., Ortiz-Monsalve, S., Mella, B., Da Costa, D., Poll, E. & Gutterres, M. 2017 Fungal biomass as biosorbent for the removal of Acid Blue 161 dye in aqueous solution. *Environmental Science and Pollution Research* **24** (4), 4200–4209.

Sabna, V., Thampi, S. G. & Chandrakaran, S. 2016 Adsorption of crystal violet onto functionalised multi-walled carbon nanotubes: equilibrium and kinetic studies. *Ecotoxicology and Environmental Safety* **134** (1), 390–397.

Sen, S. K., Raut, S., Bandyopadhyay, P. & Raut, S. 2016 Fungal decolouration and degradation of azo dyes: a review. *Fungal Biology Reviews* **30** (3), 112–133.

Senthilkumaar, S., Kalaamani, P. & Subburaam, C. V. 2006 Liquid phase adsorption of Crystal violet onto activated carbons derived from male flowers of coconut tree. *Journal of Hazardous Materials* **136** (3), 800–808.

Shoukat, S., Bhatti, H. N., Iqbal, M. & Noreen, S. 2017 Mango stone biocomposite preparation and application for crystal violet adsorption: a mechanistic study. *Microporous and Mesoporous Materials* **239** (1), 180–189.

Sips, R. 1948 On the structure of a catalyst surface. *The Journal of Chemical Physics* **16** (5), 490–495.

Soltani, N., Bahrami, A., Peche Canul, M. I. & Gonzalez, L. A. 2015 Review on the physicochemical treatments of rice husk for production of advanced materials. *Chemical Engineering Journal* **264** (1), 899–935.

Souza, A. R. C., Baldoni, D. B., Lima, J., Porto, V., Marcuz, C., Ferraz, R. C., Kuhn, R. C., Jacques, R. J. S., Guedes, J. V. C. & Mazutti, M. A. 2015 Bioherbicide production by *Diaporthe* sp. isolated from the Brazilian Pampa biome. *Biocatalysis and Agricultural Biotechnology* **4** (4), 575–578.

Svecova, L., Spanelova, M., Kubal, M. & Guibal, E. 2006 Cadmium, lead and mercury biosorption on waste fungal biomass issued from fermentation industry. I. Equilibrium studies. *Separation and Purification Technology* **52** (1), 142–153.

Tahir, N., Bhatti, H. N., Iqbal, M. & Noreen, S. 2017 Biopolymers composites with peanut hull waste biomass and application for Crystal Violet adsorption. *International Journal of Biological Macromolecules* **94** (1), 210–220.

Tran, H. N., You, S. J., Hosseini-Bandegharaei, A. & Chao, H. P. 2017 Mistakes and inconsistencies regarding adsorption of contaminants from aqueous solutions: a critical review. *Water Research* **120** (1), 88–116.

Wu, F. C., Tseng, R. L. & Juang, R. S. 2009 Characteristics of Elovich equation used for the analysis of adsorption kinetics in dye-chitosan systems. *Chemical Engineering Journal* **150** (2–3), 366–373.

Zazycki, M. A., Godinho, M., Perondi, D., Foletto, E. L., Collazzo, G. C. & Dotto, G. L. 2018 New biochar from pecan nutshells as an alternative adsorbent for removing reactive red 141 from aqueous solutions. *Journal of Cleaner Production* **171** (1), 57–65.

First received 13 December 2018; accepted in revised form 22 February 2019. Available online 7 March 2019